THE JOURNAL OF BIOLOGICAL CHEMISTRY
Vol. 274, No. 30, Issue of July 23, pp. 21186–21190, 1999

Printed in U.S.A.

Visual Arrestin Activity May Be Regulated by Self-association*

(Received for publication, February 11, 1999)

Carsten Schubert‡§¶, Joel A. Hirsch‡§‖, Vsevolod V. Gurevich, Donald M. Engelman‡, Paul B. Sigler‡ ‡‡, and Karen G. Fleming‡§§**

*From the ‡Department of Molecular Biophysics and Biochemistry and ‡‡Howard Hughes Medical Institute, Yale University, New Haven, Connecticut 06520-8114 and the **Ralph and Muriel Roberts Laboratory for Vision Science, Sun Health Research Institute, Sun City, Arizona 85372*

Visual arrestin is the protein responsible for rapid quenching of G-protein-coupled receptor signaling. Arrestin exists as a latent inhibitor which must be 'activated' upon contact with a phosphorylated receptor. X-ray crystal structures of visual arrestin exhibit a tetrameric arrangement wherein an asymmetric dimer with an extensive interface between conformationally different subunits is related to a second asymmetric dimer by a local two-fold rotation axis. To test the biological relevance of this molecular organization in solution, we carried out a sedimentation equilibrium analysis of arrestin at both crystallographic and physiological protein concentrations. While the tetrameric form can exist at the high concentrations used in crystallography experiments, we find that arrestin participates in a monomer/dimer equilibrium at concentrations more likely to be physiologically relevant. Solution interaction analysis of a proteolytically modified, constitutively active form of arrestin shows diminished dimerization. We propose that self-association of arrestin may provide a mechanism for regulation of arrestin activity by (*i*) ensuring an adequate supply for rapid quenching of the visual signal and (*ii*) limiting the availability of active monomeric species, thereby preventing inappropriate signal termination.

G-protein-coupled receptor (GPCR) signaling is a ubiquitous mode of communicating information from the extracellular surroundings to the cytosol of eukaryotic cells. A wide variety of signals, ranging from light to small molecules to macromolecules, are sensed with this pathway. The signal sensor is a seven-transmembrane helical receptor protein which activates heterotrimeric G-proteins by catalyzing nucleotide exchange, enabling the G-protein subunits to associate with and modulate the action of effectors. G-protein receptor kinases and arrestins, respectively, attenuate and then quench signaling (1, 2). The arrestin family of molecules terminates the signal by binding tightly to the activated and phosphorylated receptors, occluding the competing G-proteins. In addition, in nonvisual systems, they mediate the interaction with clathrin in the endocytic sequestration of the receptor. Association of visual arrestin with rhodopsin is highly selective for light-activated and phosphorylated receptor (Rho*-P)[1] (3).

Arrestins appear to be inactive latent inhibitors whose basal conformation prevents effective interaction with the cytosolic surface of the activated receptor. The structural basis for the activation of arrestin has been elucidated by crystallographic and mutational analyses.[2,3] Contact with the C-terminal segment of phosphorylated receptor is required to activate the inhibitory action of arrestin, apparently by releasing the constraints that maintain the inactive state of arrestin thus permitting a conformational adjustment (6). Proteolytic and mutational variants can also release these constraints, resulting in a constitutively active form of arrestin that bypasses the need for contact with the phosphorylated C-terminal segment of the receptor (7).

Crystallographic studies of visual arrestin in its inactive, basal state have revealed a tetrameric quaternary structure (8)[2] in which there are two asymmetric dimers, each with an extensive internal interface between conformationally different arrestin subunits. The two asymmetric dimers are arranged in a 2-fold symmetrical tetramer. The quaternary structure was found in the asymmetric unit of two different crystal forms that were grown under markedly different conditions (8).[2] These findings led us to ask whether this oligomerization state applied to arrestin in solution and at concentrations that are likely to be physiologically relevant. In addition, the oligomerization state of arrestin ΔV8 was determined. Arrestin ΔV8 is a proteolytically modified, constitutively active form of arrestin that binds to light-activated, nonphosphorylated rhodopsin (Rho*) in addition to Rho*-P.

EXPERIMENTAL PROCEDURES

Protein Expression and Purification—Recombinant arrestin (the encoding gene contains a single glycine inserted at residue 2 of the wild-type sequence) was expressed in *Escherichia coli* strain ER2508 (New England Biolabs) using the pTrcB vector (Invitrogen) and purified by sequential heparin-Sepharose, Mono-Q (Amersham Pharmacia Biotech), and Mono-S chromatography (9, 10). Transformed ER2508 cells were grown for 4–5 h at 30 °C in 12 liters of LB containing 100 $\mu g/ml^{-1}$ ampicillin. Upon reaching an A_{600} of 0.6, cells were induced with 20–30 μM IPTG over a 17–20-h period. Cells were harvested by centrifugation and suspended in lysis buffer (20 mM Tris-HCl, pH 7.5; 100 mM NaCl; 2 mM dithiothreitol; 1 mM PMSF; 1 mM benzamidine, 2 mM EDTA, 2 mM EGTA). After lysis in a microfluidizer (Microfluidics), cell debris was

* This work was funded by National Institutes of Health Grants GM 54160 and GM 22778 (to D. M. E.) and Grant GM 22324 (to P. B. S.) and National Eye Institute Grant EY11500 (to V. V. G.). The costs of publication of this article were defrayed in part by the payment of page charges. This article must therefore be hereby marked "*advertisement*" in accordance with 18 U.S.C. Section 1734 solely to indicate this fact.

This paper is dedicated to the memory of Serge Pares, our colleague and friend.

§These authors contributed equally to this work.
¶ Is a Fellow of the Deutsche Forschungsgemeinschaft.
‖ Is a National Eye Institute Postdoctoral Fellow.
§§ To whom correspondence should be addressed: Dept. of Molecular Biophysics and Biochemistry, Yale University, P. O. Box 208114, 266 Whitney Ave., New Haven, CT 06520-8114. Tel.: 203-432-5600; Fax: 203-432-5175; E-mail: kgf@csb.yale.edu.

[1] The abbreviations used are: Rho*-P, light-activated and phosphorylated rhodopsin; Rho*, light-activated and nonphosphorylated rhodopsin; PMSF, phenylmethylsulfonyl fluoride; MES, 2-(*N*-morpholino) ethanesulfonic acid; IPTG, isopropyl-1-thio-β-D-galactopyranoside.

[2] Hirsch, J. A., Schubert, C., Gurevich, V. V., and Sigler, P. B. (1999) *Cell* **97,**257–269.

[3] Vishnivetskiy, S. A., Paz, C. L., Schubert, C., Hirsch, J. A., Sigler, P. B., and Gurevich, V. V. (1999) *J. Biol. Chem.* **274,** 11451–11454.

removed by centrifugation at 100,000 × *g*, followed by precipitation in a 50% saturated $(NH_4)_2SO_4$ solution. The precipitate was resuspended in 10 mM Tris-HCl (pH 7.5), 2 mM EDTA; 0.5 mM PMSF (C buffer). The ionic strength was adjusted to 100 mM NaCl by dialysis against C buffer containing 100 mM NaCl, and the protein was loaded onto a HiTrap heparin column (Amersham Pharmacia Biotech) equilibrated with C buffer containing 100 mM NaCl at 4 °C (flow rate = 1–1.5 ml/min^{-1}). The column was washed with C buffer containing 150 mM NaCl until a stable base line was achieved. After elution with a linear gradient of C buffer from 150 mM NaCl to 400 mM NaCl, arrestin-containing fractions (approximately 250 mM NaCl) were pooled and buffer was exchanged by ultrafiltration to 10 mM Tris-HCl (pH 8.5), 2 mM EDTA, 0.5 mM PMSF (Q buffer), with 100 mM NaCl. Immediately before loading onto a Mono-Q column (Amersham Pharmacia Biotech) (21 °C), the protein was diluted 1:5-fold with Q buffer. The column was washed with Q buffer containing 150 mM NaCl, and fractions were eluted with a shallow linear gradient of Q buffer containing 150–500 mM NaCl. Arrestin-containing fractions were pooled (180–200 mM NaCl) and concentrated, and buffer was exchanged by ultrafiltration to 10 mM Na_2HPO_4, NaH_2PO_4 (pH 6.5) (S buffer) containing 100 mM NaCl and was diluted 1:5-fold with S buffer. The diluted sample was loaded onto a Mono-S (10/10) column (Amersham Pharmacia Biotech) and eluted with a linear gradient of S buffer from 100–500 mM NaCl (eluted at 150–170 mM NaCl). As assessed by SDS-polyacrylamide gel electrophoresis, electrospray mass spectrometry and N-terminal sequencing, arrestin is > 95% pure after this step. The N-terminal methionine is cleaved *in vivo* as determined from sequencing and mass spectrometry. Following buffer exchange to 10 mM Tris-HCl, 100 mM NaCl, the pooled fractions were concentrated to 10 mg ml^{-1} using Centricons (Amicon), divided into 30-μl aliquots and flash frozen in liquid N_2.

Arrestin ΔV8 (residues 2–368 *versus* full-length 2–404) was prepared as follows. Purified recombinant arrestin was diluted to 2.5 mg/ml in 10 mM Tris-HCl (pH 7.5), 100 mM NaCl. Proteolysis was initiated by addition of *Staphylococcus aureus* V8 protease (Roche Molecular Biochemicals) at a ratio of 150:1 (by weight) of arrestin to enzyme. The digestion was performed at 4 °C for 18 h. The digested material was then diluted with an equal volume of 10 mM MES (pH 5.95), 100 mM NaCl (buffer M) and loaded onto a previously equilibrated Source S cation exchange column (Amersham Pharmacia Biotech). A linear gradient was developed (100–400 mM NaCl), and arrestin ΔV8 was eluted at approximately 250 mM NaCl. Fractions were assayed by SDS-polyacrylamide gel electrophoresis, pooled, concentrated by ultrafiltration in a buffer of 10 mM Bis-Tris (pH 6.25), 150 mM NaCl to 10 mg/ml, and frozen in 25-μl aliquots in liquid nitrogen. Some samples were further processed by gel filtration chromatography on a Superdex S75 (Amersham Pharmacia Biotech) column in buffer M at a flow rate of 0.5 ml/min. Fractions were then pooled, concentrated, and frozen as above. Samples were submitted to analysis by electrospray mass spectrometry and C-terminal sequencing to determine the precise point of cleavage by V8.

Sedimentation Equilibrium of Full-length Arrestin—A Beckman XL-I analytical ultracentrifuge was used to obtain the equilibrium distribution of bovine arrestin at seven initial concentrations and at eight speeds in buffer containing 10 mM Tris, 100 mM NaCl at pH 8.5. The buffer conditions were chosen to reflect the crystallization conditions[2] and are near the physiological range (NaCl substituted for KCl). The protein concentration was detected using the absorbance optics at either 250 or 280 nm, chosen so that the absorbance would fall within the linear range. Six initial concentrations were evaluated ranging from 9 to 62 μM (.40–2.8 mg/ml) at 4 °C. Rotor speeds were 7000, 8800, 10,800, 13,300, 16,300, 20,000, 24,500, and 30,000 rpm. Sample setups for these six concentrations were carried out using standard six-sector cells equipped with quartz windows. Sample volumes were 110 μl. Data at 16 °C and 37 °C were collected for the same concentrations at rotor speeds of 16,300 and 20,000 rpm. An additional initial concentration of 220 μM (10 mg/ml) was examined using a two-sector cell equipped with spacers and a 0.3-mm path-length centerpiece (37-μl sample volume). Sedimentation equilibrium was established using the algorithm MATCH. The Windows 95 version of NONLIN (11) was used to analyze sedimentation equilibrium data to obtain estimates for the association states and equilibrium constants. Values for the protein partial specific volume at each temperature were calculated from the amino acid composition using SEDNTERP, which is based on the method of Laue (12). They were 0.7346, 0.7397, 0.7486 ml g^{-1} at 4, 16, and 37 °C, respectively. The solvent densities at each temperature were also calculated using SEDNTERP. They were 1.00452, 1.00349, and 0.99785 g/ml^{-1} at 4, 16, and 37 °C, respectively. Data in absorbance units were converted to molar concentrations using molar extinction coefficients of 26,360 at 280 nm and 9922 at 250 nm for a 1-cm path-length, also calculated using SEDNTERP.[4]

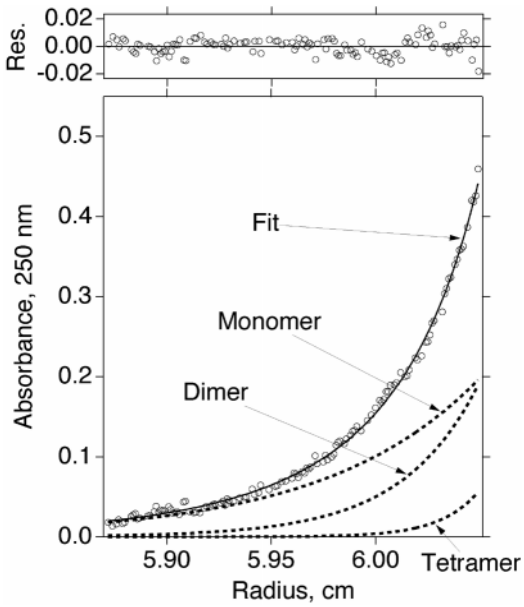

FIG. 1. **Sedimentation equilibrium distribution of 2.8 mg/ml arrestin at 20,000 rpm.** The *circles* in the *lower panel* are the data points, and the *solid line* is the global fit to a monomer/dimer/nonequilibrating tetramer model (Equation 1) as described under "Results." The *dotted lines* represent the exponentials whose sum gives rise to the fit. The residuals of the fit (Abs_{fit}-Abs_{obs}) are shown in the *upper panel*.

Analysis of Arrestin ΔV8—A Beckman XL-I analytical ultracentrifuge was used to obtain the equilibrium distribution of bovine arrestin ΔV8 at three initial concentrations and at four speeds in buffer containing 10 mM Tris, 100 mM NaCl at pH 8.5. The protein concentration was detected using the absorbance optics at 280 nm so that the absorbance would fall within the linear range. Three initial concentrations were evaluated ranging from 16 to 40 μM at 4 °C. Rotor speeds were 16,300, 20,000, 24,500, and 30,000 rpm. Sample setups and data analysis were carried out using standard procedures given above. The values for the protein partial specific volume (0.7476 ml/g^{-1}) and the solvent density (1.00452 g/ml^{-1}) were calculated using SEDNTERP. Data in absorbance units were converted to molar concentrations using a molar extinction coefficient of 24,870 at 280 nm for a 1-cm path-length, which was also calculated using SEDNTERP.

RESULTS

Arrestin Participates in a Monomer/Dimer Equilibrium at Physiological Concentrations—The self-association propensity for visual arrestin at micromolar concentrations was investigated using sedimentation equilibrium. A global nonlinear least squares analysis of 15 data sets collected at six initial concentrations and three speeds was carried out using NONLIN. The results of fitting trials suggest that the simplest model that adequately describes the data contains three species with molecular weights corresponding to an arrestin monomer, dimer, and tetramer. A typical distribution is shown in Fig. 1. The formal expression,

$$c_i = c_{ref}\exp[\sigma(\xi_i - \xi_{ref})] + c_{ref}^2 K_{1,2}\exp[2\sigma(\xi_i - \xi_{ref})] + c_{ref}^4 K_{1,4}\exp[4\sigma(\xi_i - \xi_{ref})] + base \quad \text{(Eq. 1)}$$

[4] The software programs MATCH, SEDNTERP, and NONLIN are available as shareware from the RASMB web site at http://www.bbri.org/rasmb/rasmb.html.

where c_i is the total absorbance at a radial position, r_i; c_{ref} is the monomer absorbance at a reference position, r_{ref}; $\sigma = M(1 - \bar{\nu}_{Pr}\rho)\omega^2/RT$; M is the monomer molecular mass; $\bar{\nu}_{Pr}$ is the monomer partial specific volume; ρ is the solvent density; ω is the angular velocity (radians sec^{-1}); R is the universal gas constant; T is the absolute temperature; $\xi = r^2/2$; $K_{1,2}$ is the monomer-dimer equilibrium constant (in absorbance units) that was common for all data sets, $K_{1,4}$ is the apparent monomer-tetramer equilibrium constant that was different for each data set, and *base* is a base-line term for nonsedimenting material.

The fit was judged to be good by examination of the residuals (small and random) and minimization of the variance (5.17×10^{-3} with 1443 degrees of freedom). A value of 34 ($\pm$4) μM for the dimer/monomer dissociation equilibrium constant was determined from this global fit using Equation (1). Attempts to globally fit the data using a fitting function containing a common tetramer/dimer dissociation constant for all data sets failed to converge as indicated by non-randomness of the residuals (data not shown) and a significant increase in the variance (6.25×10^{-3} with 1454 degrees of freedom). The global analysis thus suggests that the tetramer is not reversibly associating with the other species on the time scale of this experiment and so is taken as thermodynamically heterogeneous. The tetramer concentration is low (Fig. 1).

Temperature Dependence of Arrestin Dimerization—To obtain additional information on the thermodynamics of arrestin dimerization, the temperature dependence of arrestin self-association was examined by sedimentation equilibrium experiments carried out at 16 and 37 °C. Twelve data sets (six concentrations at two speeds each) at each temperature were used in a global analysis of the equilibrium data. At both temperatures, Equation (1) was found to best describe the arrestin equilibrium distributions. Dimer/monomer dissociation constants were estimated to be 26 ($\pm$5) μM at 16 °C and 30 ($\pm$5) μM at 37 °C. The temperature dependence of the equilibrium constant using an Arrhenius analysis shows that the association enthalpy change is too small to be measured over the experimentally accessible temperature range.

Arrestin Can Form Tetramers at High Concentrations—To determine the oligomeric state of arrestin at crystallographic concentrations, sedimentation equilibrium experiments were conducted on a highly concentrated sample (10 mg/ml) using small path-length cells. The simplest model that adequately describes the data contains two noninteracting species. The formal expression is,

$$c_i = c_{ref,tet}\exp[4\sigma(\xi_i - \xi_{ref})] + c_{ref,nmer}\exp[n\sigma(\xi_i - \xi_{ref})] + base \quad \text{(Eq. 2)}$$

where the symbols are as described as above. The best fit value for n was found to be 12. Thus, the higher order species corresponds to an arrestin dodecamer. Inclusion of a nonideality term did not lead to significant improvements in the fit. As can be seen from Fig. 2, the tetramer was found to be the predominant species in solution under these conditions. The fit also notes the absence of lower oligomeric species (such as the dimer), which is consistent with the thermodynamically heterogeneous behavior of the arrestin tetramer.

Solution Interaction Analysis of Arrestin Δ*V8*—Arrestin ΔV8 is a proteolyzed form of arrestin produced by digestion with *S. aureus* V8 protease, an endopeptidase that cleaves the peptide bond on the carboxylic side of glutamate residues. Electrospray mass spectrometry in conjunction with C-terminal peptide sequencing determined that arrestin ΔV8 comprises residues

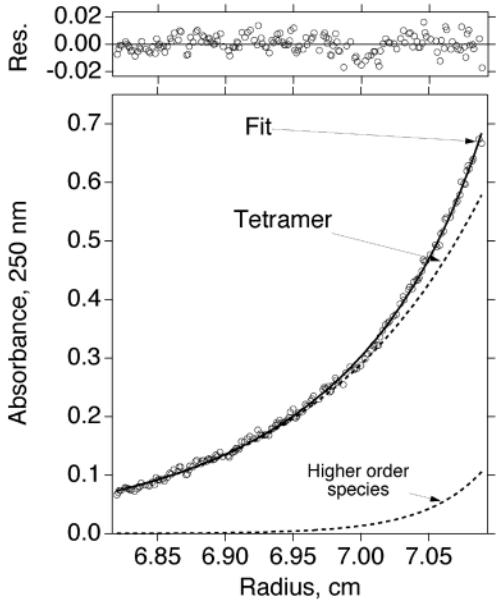

FIG. 2. **Sedimentation equilibrium distribution of 10 mg/ml arrestin at 7000 rpm.** The *open circles* in the *lower panel* are the data points, and the *solid line* is the fit to a nonequilibrating tetramer/dodecamer model (Equation 2) as described under "Results." The *dotted lines* represent the exponentials whose sum gives rise to the fit. The residuals of the fit (Abs_{fit}-Abs_{obs}) are shown in the *upper panel*. Note that the absorbance values at 250 nm are reported as measured by the 3-mm path-length used in this experiment.

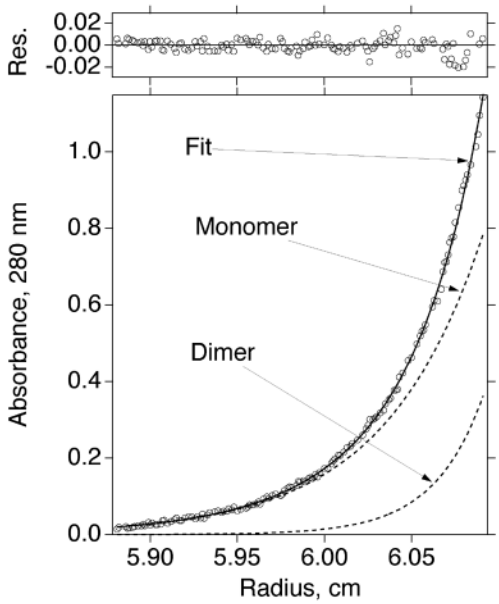

FIG. 3. **Sedimentation equilibrium distribution of arrestin 1.6 mg/ml ΔV8 at 24,500 rpm.** The *circles* in the *lower panel* are the data points, and the *solid line* is the global fit to a monomer/dimer/nonequilibrating tetramer model (Equation 1) as described under "Results." The *dotted lines* represent the exponentials whose sum gives rise to the fit. The residuals of the fit (Abs_{fit}-Abs_{obs}) are shown in the *upper panel*.

2–368. (The N-terminal methionine is cleaved in the bacterial expression system.) Arrestin ΔV8 binds significantly to both Rho*-P and Rho*. Such a binding profile is identical with that of engineered recombinant C-terminal truncations of similar segments and indicates an active conformation.

A global nonlinear least squares analysis of twelve data sets collected at three initial concentrations and four speeds was carried out using NONLIN. The results of fitting trials show that the simplest model that adequately describes the data

contains three species with molecular weights corresponding to an arrestin ΔV8 monomer, dimer, and tetramer (Equation 1). A distribution of species is given in Fig. 3. The tetramer was present in small amounts (<10%) in the observed concentration range. The fit was judged to be good by examination of the residuals (small and random) and minimization of the variance (5.48×10^{-3} with 1311 degrees of freedom). A value of 114 (±5) μM for the dimer/monomer dissociation equilibrium constant was determined from a global fit of the data using Equation 1. Attempts to globally fit the data using a fitting function containing a common tetramer/dimer dissociation constant for all data sets failed to converge as indicated by non-randomness of the residuals (data not shown) and a significant increase in the variance (6.14×10^{-3} with 1318 degrees of freedom). The global analysis thus suggests that the tetramer is not reversibly associating with the other species on the time scale of the experiment. This behavior is similar to that observed for the full-length arrestin protein.

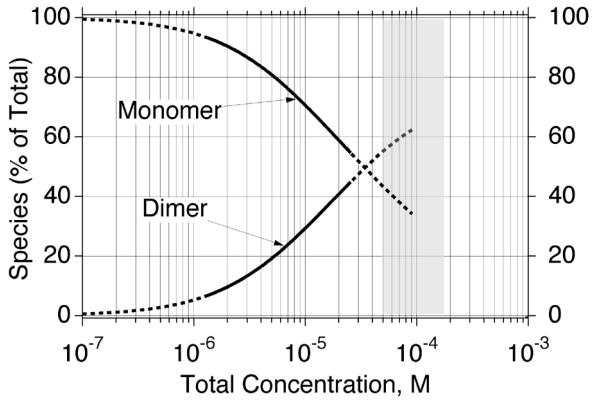

FIG. 4. **Monomer/dimer species distribution of arrestin.** The distribution of monomeric and dimeric species are calculated as a function of total molar concentration from the estimated equilibrium constant at 4 °C. The *solid portions* of the *curves* represent the concentration range wherein the equilibrium analysis was carried out. The *broken portions* of the *curves* are extrapolations of those data. The *shaded portion* of the graph indicates the estimated biological concentration range for arrestin in rod outer segments.

DISCUSSION

Arrestin is the second most abundant soluble protein in rod outer segments. By comparison to rhodopsin and transducin (G_t) concentrations, it is estimated that the physiological concentration of arrestin is in the range of 50–170 μM (13, 14). Fig. 4 shows the concentration-dependent distribution of oligomeric species for the thermodynamically homogeneous monomer and dimer arrestin forms. Extrapolation of the distribution reveals that arrestin is monomeric at micromolar concentrations and below. The distribution is poised such that the monomer/dimer ratio of arrestin would be 45:55% in the biologically relevant concentration range. However, this estimate of the monomer fraction is an upper limit due to excluded volume effects *in vivo*.

As stated in the introduction, arrestin appears as a dimer of dimers in the crystalline state (Fig. 5A) (8).[2] The protomeric dimer is a heterodimer of arrestins having similar overall folds but distinctly different local conformations. We call the dimer subunits α and β. The α′β′ dimer is thus related by a noncrystallographic two-fold rotation axis to αβ. As described in detail in the structure report,[2] arrestin has a bipartite architecture, divided into an N-domain (N for N-terminal; residues 1–179) and a C-domain (C for carboxyl terminal; residues 184–362) with a C-tail (residues 372–404).

The question then arises: what is the quaternary structure in solution? Close inspection of the molecular arrangement in the crystal structure reveals that there are three possible permutations for dimerization. The permutations are 1) α and β, head to tail, *i.e.* the C-domain of one molecule interacts with the N-domain of the other (Fig. 5*B*); 2) α′ and β, tail to tail, *i.e.* the C-domain of one molecule interacts with the C-domain of the other (Fig. 5*C*); and 3) β and the crystallographic symmetry mate of β′, head to head, *i.e.* the N-domain of one molecule interacts with the N-domain of the other (Fig. 5*D*). Computation of the total buried surface due to dimerization would strongly favor either permutation one or three (~2000 Å^2) *versus* permutation two (~1000 Å^2). For reasons explained

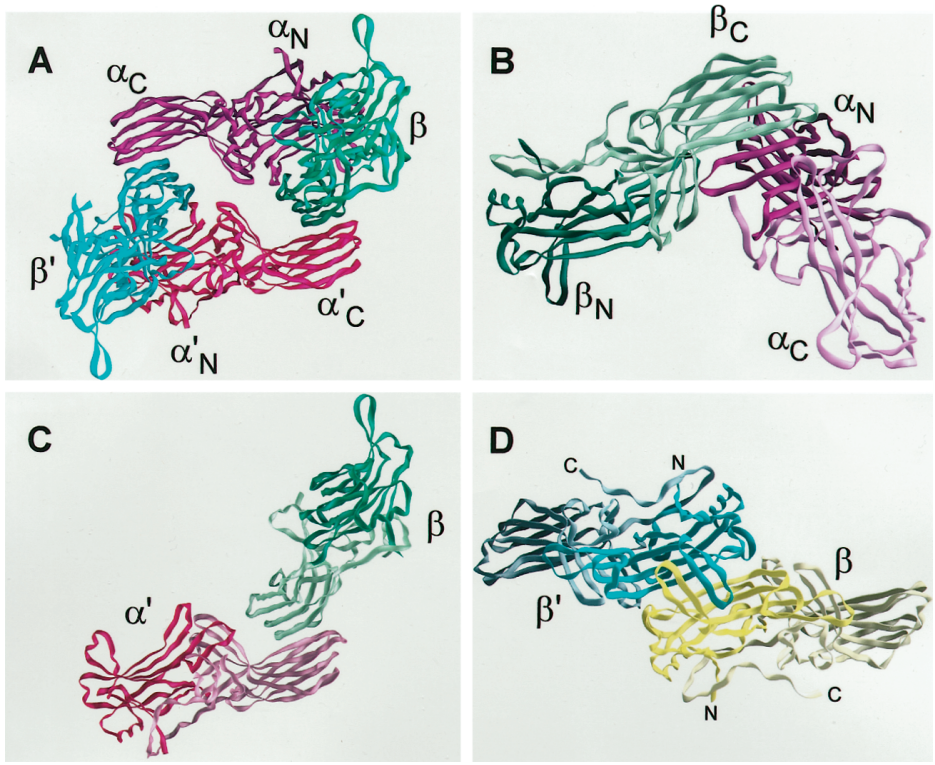

FIG. 5. **Dimer permutations.** *A*, depiction of the tetramer from the asymmetric unit of the crystal structures. The view is down the noncrystallographic 2-fold rotation axis. The N- and C-domains of the α and α′ subunits are labeled. Domain labels for the β and β′ subunits have been omitted for clarity. Shown are possible dimer configurations. *B*, permutation one (αβ): head to tail configuration. α is colored *magenta* whereas β is colored *green*. The N- and C-domains of both subunits are labeled. *Dark hues* indicate the N-domains (heads) and *lighter hues* indicate the C-domains (tails). *C*, permutation two (α′β): tail to tail configuration. The orientation is close to that viewed in *panel A*. Domain labels have been omitted for clarity. Differing hues indicate domains as in *panel B*. *D*, permutation three (ββ′): head to head configuration. Domain labels have been omitted for clarity. *Brighter hues* indicate N-domains (heads). The N and C termini are labeled. The figure was generated with GRASP (5).

below, we favor permutation one ($\alpha\beta$).

The dimer interface between α and β involves two loci of interactions. One region is a parallel strand-strand interaction, forming a continuous sheet from one molecule to the next. This area extends for ten residues of the main chain and also involves side chain interactions with several van der Waals contacts and hydrogen bonding. The second region is less extensive in terms of hydrogen bonds but is noteworthy because of its unusual interclasping of rolled sheet surfaces. Analysis by the method of Richards (15) gives a value of 2100 Å^2 total surface area that is buried upon dimerization of α and β. This value is in the range thought to represent *bona fide* dimers (16) as opposed to the much smaller values (<800 Å^2) which arise due to crystal packing.

Crystallographic and mutational analysis have implicated the C-tail as a central component in stabilizing the inactive, basal state of arrestin by contributing to the N- and C-domain interface of arrestin. Consequently, removal of the C-tail either in a natural splice variant (p^{44}), by proteolysis, or by engineered recombinant truncations relaxes the discrimination of arrestin against nonphosphorylated, activated receptor, allowing significant binding to both Rho* and Rho*-P (17–19). The proposal that arrestin oligomers are comprised of inactive, basal state molecules[2] leads to the hypothesis that the C-tail might also play an indirect role in stabilizing oligomerization of arrestin by supporting stable domain interactions of the inactive state. Such a stable conformation may better enable head to tail dimer formation (permutation one) *versus* the head to head configuration of permutation three. To test the possible role of the C-tail in oligomerization, we carried out solution interaction analysis of a constitutively active arrestin form, arrestin ΔV8, which lacks the C-tail. Consistent with similar arrestin forms, *e.g.* p^{44}, receptor binding experiments with arrestin ΔV8 demonstrate its ability to bind to both Rho* and Rho*-P (data not shown). Our solution interaction analysis studies reveal a nearly 4-fold reduction in association propensity for this proteolytic form. This result strongly suggests that the C-tail not only stabilizes the basal state through its myriad of interactions with the N- and C-domains, but as a consequence, also plays a role in stabilizing oligomerization.

Since rhodopsin binding experiments are performed with nanomolar concentrations of arrestin, well within the monomeric regime (Fig. 4), arrestin must be competent to undergo its conformational changes to bind Rho*-P as a monomer (20). Why then does arrestin self-associate? Because the structure suggests that arrestin oligomers are comprised of inactive, basal state molecules,[2] we propose that regulation of arrestin activity by self-association may provide a mechanism to limit the concentration of arrestin capable of activation in the cell. In this sense, the dimeric form of arrestin might then represent a "storage" form of the protein, which could be quickly mobilized by dissociation to meet increased needs for terminating the visual signal. Furthermore, the tetramer may represent a long term storage form, because its dissociation is characterized by a much longer time scale. At the same time, oligomerization prevents potentially high concentrations of monomeric arrestin from dampening a receptor response inappropriately.

A biological precedent for self-association playing a negative regulatory role can be found in the case of TATA binding protein (TBP), a general transcription factor. In that case, TBP is primarily an inactive homodimer in solution (4, 21, 22). Upon dissociation, it binds to its target DNA sequence, the TATA box, located approximately 35 nucleotides upstream from the start site of transcription. When bound to DNA, TBP serves as the nucleating molecule for assembly of the transcription machinery. It has been proposed that dimerization is a storage mechanism, providing a readily accessible supply for immediate transcription initiation. Moreover, in a manner parallel with arrestin, TBP dimerization may prevent adventitious binding to promoters and therefore potentially undesirable nucleation of preinitiator assemblies.

In summary, we have shown using analytical ultracentrifugation that visual arrestin at *in vivo* concentrations will have a monomer/dimer distribution. The dominant species *in vivo* will most likely be a dimeric "storage" form. The C-tail, an important functional segment of the molecule, stabilizes self-association of the inactive form. Dimerization of arrestin therefore furnishes a mechanism for its self-regulation.

Acknowledgment—We thank Joe Leykam of Michigan State University for C-terminal sequencing.

REFERENCES

1. Krupnick, J. G., and Benovic, J. L. (1998) *Annu. Rev. Pharmacol. Toxicol.* **38,** 289–319
2. Lefkowitz, R. J. (1998) *J. Biol. Chem.* **273,** 18677–18680
3. Gurevich, V. V., Dion, S. B., Onorato, J. J., Ptasienski, J., Kim, C. M., Sterne-Marr, R., Hosey, M. M., and Benovic, J. L. (1995) *J. Biol. Chem.* **270,** 720–731
4. Coleman, R. A., and Pugh, B. F. (1997) *Proc. Natl. Acad. Sci. U. S. A.* **94,** 7221–7226
5. Nicholls, A., Sharp, K., and Honig, B. (1991) *Proteins* **11,** 281–296
6. Palczewski, K. (1994) *Protein Sci.* **3,** 1355–1361
7. Gurevich, V. V., and Benovic, J. L. (1997) *Mol. Pharmacol.* **51,** 161–169
8. Granzin, J., Wilden, U., Choe, H. W., Labahn, J., Krafft, B., and Buldt, G. (1998) *Nature* **391,** 918–921
9. Gray-Keller, M. P., Detwiler, P. B., Benovic, J. L., and Gurevich, V. V. (1997) *Biochemistry* **36,** 7058–7063
10. Gurevich, V. V., Pals-Rylaarsdam, R., Benovic, J. L., Hosey, M. M., and Onorato, J. J. (1997) *J. Biol. Chem.* **272,** 28849–28852
11. Johnson, M. L., Correia, J. J., Yphantis, D. A., and Halvorson, H. R. (1981) *Biophys. J.* **36,** 575–588
12. Laue, T. M., Shah, B., Ridgeway, T. M., and Pelletier, S. L. (1992) in *Analytical Ultracentrifugation in Biochemistry and Polymer Science* (Harding, S. E., Rowe, A. J., and Horton, J. C., eds), pp. 90–125, Royal Society of Chemistry, Cambridge, UK
13. Hamm, H. E., and Bownds, M. D. (1986) *Biochemistry* **25,** 4512–4523
14. Kawamura, S. (1995) in *Neurobiology and Clinical Aspects of the Outer Retina* (Djamangoz, M. B. A., Archer, S. N., and Vallerga, S., eds), pp. 105–131, Chapman & Hall, London
15. Lee, B., and Richards, F. M. (1971) *J. Mol. Biol.* **55,** 379–400
16. Jones, S., and Thornton, J. M. (1995) *Prog. Biophys. Mol. Biol.* **63,** 31–65
17. Palczewski, K., Buczylko, J., Ohguro, H., Annan, R. S., Carr, S. A., Crabb, J. W., Kaplan, M. W., Johnson, R. S., and Walsh, K. A. (1994) *Protein Sci.* **3,** 314–324
18. Gurevich, V. V., Chen, C. Y., Kim, C. M., and Benovic, J. L. (1994) *J. Biol. Chem.* **269,** 8721–8727
19. Gurevich, V. V. (1998) *J. Biol. Chem.* **273,** 15501–15506
20. Gurevich, V. V., and Benovic, J. L. (1993) *J. Biol. Chem.* **268,** 11628–11638
21. Coleman, R. A., Taggart, A. K. P., Benjamin, L. R., and Pugh, B. F. (1995) *J. Biol. Chem.* **270,** 13842–13849
22. Taggart, A. K., and Pugh, B. F. (1996) *Science* **272,** 1331–1333